

Fraction of stopped K^- mesons which interact with free hydrogen in propane*

C. T. Murphy,† G. Keyes, M. Saha,‡ and M. Tanaka
Carnegie-Mellon University, Pittsburgh, Pennsylvania 15213
 (Received 10 October 1973)

In a sample of film containing 13 400 stopped K^- mesons in a liquid-propane bubble chamber, 98 examples of the reaction $K^-p \rightarrow \Sigma^- \pi^+$ were found. Using the known branching ratio for this channel, we find the fraction of K^- which interact at rest with free protons to be $(3.2 \pm 0.4)\%$. The result is compared with measurements of the same fraction for π^- mesons and anti-protons.

I. INTRODUCTION

It has been known for many years¹ that the fraction of negative muons and pions which are captured at rest on hydrogen in mixtures and compounds disagrees strongly with the Z law of Fermi and Teller.² In particular, a series of experiments by Krumshtein *et al.*³ with π^- stopping in various hydrocarbons showed that the fraction of π^- which charge-exchanged on hydrogen was of the order of 1%, compared to ~20% predicted by the Z law. Krumshtein *et al.* showed that their data were in reasonable agreement with the large-mesonic-molecule model of Ponomarev.⁴

The model of Ponomarev contains no dependence on the mass of the stopping negative particle and hence predicts equal hydrogen capture probabilities for π^- mesons, K^- mesons, and antiprotons in hydrocarbons. This prediction was shown to be wrong by Pawlewicz *et al.*,⁵ who found that the hydrogen capture probability for antiprotons in propane (C_3H_8) was $(11 \pm 3)\%$. They suggested that the large difference between the behavior of π^- mesons and antiprotons might be explained by the transfer mechanism first proposed by Panofsky *et al.*,¹ an effect which is omitted from the large-mesonic-molecule model. Many π^- mesons which are captured in atomic orbits about protons could be subsequently transferred to carbon atoms in collisions before undergoing charge exchange with the proton. Antiprotons, however, might be expected to transfer less frequently, since the $\bar{p}p$ interaction is much stronger than the π^- charge-exchange reaction, and the \bar{p} wave function overlaps the nucleus at much higher values of the principal quantum number than does the π^- .

It is therefore of considerable interest to measure the same capture probability for the K^- meson. Like the antiproton, it "annihilates" very easily via hyperon production; however, it has about half the mass of the antiproton and hence might take longer to cascade down to orbits which

overlap the proton.

This paper describes a measurement of that capture probability in propane. To identify K^- interactions on free protons, the reaction $K^-p \rightarrow \Sigma^- \pi^+$ was used. Our result is in agreement with that of VanderVelde-Wilquet *et al.*,⁶ who used a slightly different technique in a mixture of hydrocarbons which was mostly propane.

II. EXPERIMENTAL PROCEDURE

The Michigan-Argonne heavy-liquid bubble chamber was exposed to a separated beam of K^- mesons at the Argonne Zero Gradient Synchrotron (ZGS). The beam entered the chamber liquid with a momentum of about 500 MeV/c and came to rest in the lower-center region of the chamber. The magnetic field was 45 kG. About 400 000 pictures were obtained, of which 11 000 were used for this study.⁷

A. Scanning

The film was scanned for beam tracks which interacted in a restricted fiducial volume and produced a π^+ and zero or more other tracks. A π^+ was defined as any track with positive curvature, longer than 4 cm in at least one view, which either stopped in the chamber and produced the well-known $\pi^+ \rightarrow \mu^+ \rightarrow e^+$ decay chain or did not appear to be a slow proton (a proton being defined as a track with no gaps and with curvature smaller than the beam track). In the sample of nonstopping π^+ , a background of fast protons was easily removed after measurement of the events (see Sec. II E).

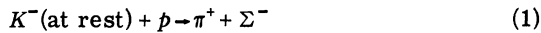
The scanner also eliminated events whose beam tracks scattered in the last 16 cm or had ending momentum greater than 260 MeV/c, as determined by a three-point template. On every twentieth frame, the same scanner counted all beam tracks interacting or decaying in the fiducial volume, subject to the same two cuts (for further discus-

sion, see Sec. II G).

A rescan of 1000 frames was performed from which the single scan efficiency was determined to be $(94 \pm 3)\%$.

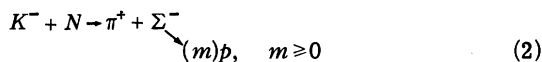
B. Editing

The scanning produced 14 000 candidates, most of which were obviously not candidates for the reaction



for a variety of reasons (e.g., the number of outgoing tracks was not two). From conservation of momentum and energy, reaction (1) should produce a π^+ with a momentum of 173 MeV/c (range 43 cm), collinear with a Σ^- which either comes to rest with a range of 0.33 cm and is captured by a carbon or hydrogen nucleus, or which decays in flight into a π^- and a neutron at a distance less than 0.33 cm from the production vertex. In this experiment, half of the events should fall into each category. However, some sizable fraction of the $\Sigma^- \rightarrow \pi^- n$ decays will be unobserved because the Σ^- track is very short or the decay angle is small, leading to the appearance that the final state is a $\pi^+ \pi^-$ pair.

Therefore, a physicist reduced the sample to be measured by the use of the following rules: (1) There must be two and only two outgoing tracks, one of which is possibly a π^+ ; (2) the second track must be either a π^- or a straight, dark track of length less than 1.0 cm and greater than 0.1 cm which produces nothing, dark prongs,⁸ or a π^- . No restriction was placed on the apparent collinearity of the Σ^- and π^+ tracks in order to collect a sample of carbon-produced and in-flight K^- background. In summary, events from three topologies were measured:



where N is either a carbon or hydrogen nucleus. These topologies are called Σ^- -stop events, Σ^- -decay events, and $\pi^+ \pi^-$ events, respectively.

These editing rules when applied to half of the film produced 591 candidates for reaction (1). An additional 101 candidates were obtained from the second half of the film by omitting topology (4) and by restricting the Σ^- track length to less than 0.6 cm and requiring visual collinearity of the Σ^- and π^+ tracks.

C. Measuring

The best three of the four available views of the events were measured on a film-plane digitizing microscope built by Nuclear Research Instruments. The measurements were processed by the geometrical reconstruction program TVGP.⁹ All events were remeasured until they either passed the goodness-of-fit criteria¹⁰ of TVGP or could be eliminated as candidates for reaction (1) on the basis of the well-measured tracks.

For TVGP, the turning angle of the measured portion of the π^+ track was restricted to 90° , since for larger angles the spiral fit (with linear energy loss) of TVGP increasingly fails. However, a π^+ with momentum 173 MeV/c actually turns through $\sim 270^\circ$ in the 45-kG magnetic field before coming to rest, allowing a determination of the momentum-by-range to an accuracy¹¹ of 1.7 MeV/c compared to about a 7-MeV/c error in the momentum-by-curvature from TVGP. Therefore, all events were also processed by the geometrical reconstruction program SHAPE,¹² which was especially designed to measure the range of a particle which spirals through many turns. SHAPE also produced a momentum-by-curvature based on the full length of a track turning through more than 90° , using a segmentation method, the result of which was used if the error in momentum from SHAPE was smaller than that of TVGP by more than a factor of 1.5. Consistency between SHAPE and TVGP was, of course, demanded. A handful of events with a stopping π^+ in which the momentum-by-range of SHAPE disagreed with the momentum-by-curvature of TVGP by more than two standard deviations were resolved after examination on the scan table.

Typical errors in the angles of the tracks involved (resulting from multiple scattering and a setting error of 0.03 cm) were 1.4° and 1.5° in the azimuth and dip of the π^+ , respectively, and 5° and 20° in the azimuth and dip of a Σ^- of length 0.3 cm (see Sec. IID).

D. Event selection

The following cuts were made on the measured sample of events:

(1). The dip of the π^+ was required to be less than 60° . This cut was necessary to assure the visibility of the short, collinear Σ^- track and also to reduce the error in the momentum by curvature of the π^+ .

(2). The length of the π^+ was required to be greater than 8 cm in order to reduce the error in the momentum by curvature.

(3). The relative azimuth of the K^- and π^+ tracks was required to lie between 18° and 162° ,

to assure that the interaction vertex was measurable.

(4). For the Σ^- -decay events, the cosine of the space angle between the Σ^- and the decay π^- was required to lie between -0.9 and $+0.9$, to assure that the decay vertex was measurable.

(5). The variable K_t for the K^- track,¹³ which should have a mean of zero and a variance of 1 for a pure sample of stopped K^- 's, was required to be less than 3. This cut eliminated K^- interactions with $P_K \geq 210$ MeV/c.

To separate Σ^- productions by stopped K^- on free hydrogen from various backgrounds, two χ^2 variables were computed for each event belonging to topology (2) or (3):

$$\chi_{\text{col}}^2 = \frac{(\lambda_{\pi^+} + \lambda_{\Sigma^-})^2}{\Delta\lambda_{\pi^+}^2 + \Delta\lambda_{\Sigma^-}^2} + \frac{(\phi_{\pi^+} - \phi_{\Sigma^-} - \pi)^2}{\Delta\phi_{\pi^+}^2 + \Delta\phi_{\Sigma^-}^2},$$

$$\chi_3^2 = \chi_{\text{col}}^2 + \frac{(P_{\pi^+} - 173)^2}{\Delta P_{\pi^+}^2}.$$

In the above equations, λ_i is the dip angle of particle i with an error $\Delta\lambda_i$, ϕ_i is the azimuth with an error $\Delta\phi_i$, and P_{π^+} is the momentum of the π^+ with an error ΔP_{π^+} . χ_{col}^2 is zero for a perfectly collinear event and χ_3^2 is zero for a collinear event with $p_{\pi^+} = 173$ MeV/c.

Figure 1 shows the π^+ momentum spectrum separately for the stopped and nonstopped π^+ . The cross-hatched region of each histogram corresponds to events with $\chi_{\text{col}}^2 \geq 6.5$. The strong signal around 173 MeV/c is evident.

Final selection of events is based on Fig. 2, which shows the distribution of χ_3^2 separately for stopped and nonstopped π^+ . The 98 events in the peaks at $\chi_3^2 < 8$ are taken to be examples of reaction (1), with background yet to be subtracted.

The events with $\chi_3^2 < 8$ in Fig. 2 all lie in the momentum regions indicated by the double arrows in Fig. 1. The root-mean-square half width of the momentum distribution for the 60 events having a stopped π^+ is 1.9 MeV/c, in good agreement with the straggling error of 1.7 MeV/c estimated by Sternheimer.¹¹ The peak in Fig. 1(a) is centered exactly on 173 MeV/c because these events were used to calibrate the density of the propane.

Figure 3 shows the structure of the peak in the χ_3^2 distribution for all events. A χ^2 distribution for three degrees of freedom should have half the events at $\chi^2 < 2.4$, which is not the case for our sample. The median occurs at $\chi_3^2 = 1.6$, suggesting that errors have been overestimated by a factor $(\frac{3}{2})^{1/2}$. The superimposed curve on Fig. 3 is the expected χ^2 distribution for three degrees of freedom, plotted against $0.66\chi_3^2$, and is a good fit to the data. The fraction of events lost be-

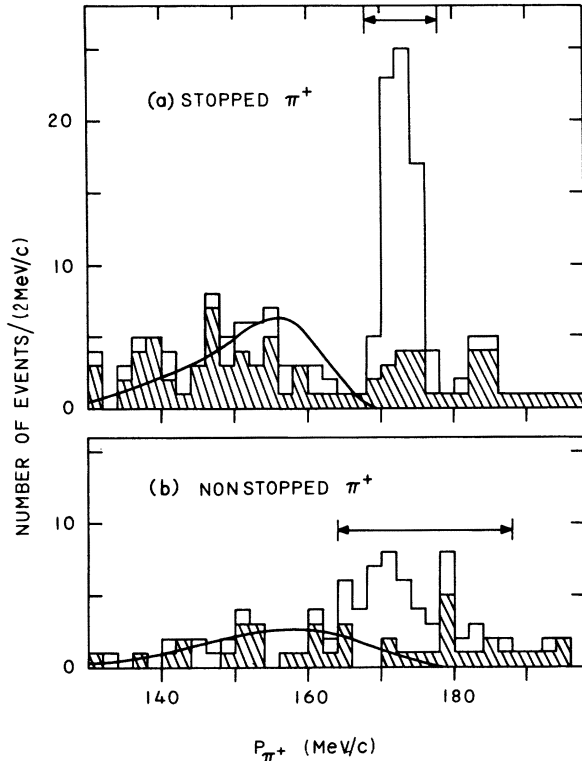


FIG. 1. Histogram of the momentum distribution of the π^+ for (a) events in which the π^+ stopped in the chamber, and (b) events in which the π^+ interacted in flight or left the chamber. Both Σ^- -stop events and Σ^- -decay events are included. The cross-hatched events failed the test for the collinearity of the Σ^- and π^+ tracks, $\chi_{\text{col}}^2 \leq 6.5$. The curve superimposed on each histogram is the prediction of an impulse model for Σ^- production on carbon discussed in Sec. II E.

cause of the cut at $\chi_3^2 = 8$ is predicted to be $(0.5 \pm 0.2)\%$.

Of the 98 events passing all selection criteria, 63 were Σ^- -stop events [reaction (2)] and 35 were Σ^- -decay events [reaction (3)]. No differences were observed between these two samples in their distributions of π^+ momentum or χ_3^2 , so they have not been distinguished in Fig. 1 and Fig. 2.

The distributions of the length of the Σ^- track shown on Fig. 4 for the two types of events do, however, differ significantly, as expected. For the Σ^- -stop events, the length distribution is consistent with the resolution function,¹⁴ but is centered at 0.36 cm compared to the value of 0.33 cm predicted by the range-energy relation. This discrepancy was traced to a misconception on the part of the measurer, who took the end of the track to be the extremity of the photographic image instead of one-half the track width from the end of the image. The shift of 0.03 cm agrees

well with the measured track widths of heavily ionizing particles in this film.

In contrast to the Σ^- -stop events for which an over-all scale factor in the length distribution does not affect the analysis, it is important to have no bias in the track lengths for the Σ^- -decay events to facilitate a correction for the loss of events in which the Σ^- decayed very close to the production vertex. Since the original measurements of the Σ^- -decay events had overestimated the Σ^- track lengths, all of these events were remeasured with a high density of points on each track near the production and decay vertices. The vertices on each view were then found from the intersections of circles fitted to the K^- and π^- tracks with a straight line fitted to the Σ^- track. The length distribution resulting from these measurements is shown in Fig. 4(b). The superimposed curve will be discussed in Sec. II F.

In half of the film, 340 $\pi^+\pi^-$ events [reaction (4)] were measured in an attempt to detect the short Σ^- -decay events missing from Fig. 4(b). The signal-to-background ratio in the π^+ momen-

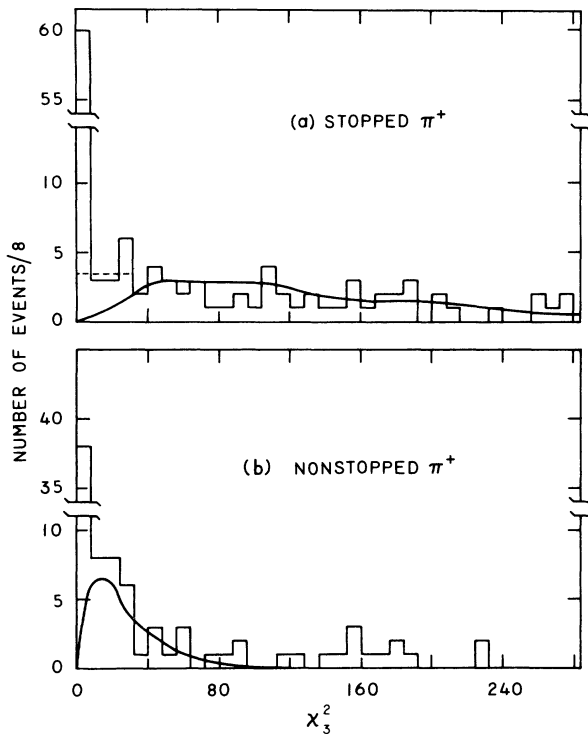


FIG. 2. Histogram of the distribution of χ_3^2 , the χ^2 for the three-constraint fit to the hypothesis that the event is reaction (1). (a) Events in which the π^+ stopped in the chamber; (b) events in which the π^+ interacted in flight or left the chamber. The curve superimposed on each histogram is the prediction of an impulse model for Σ^- production on carbon discussed in Sec. II E.

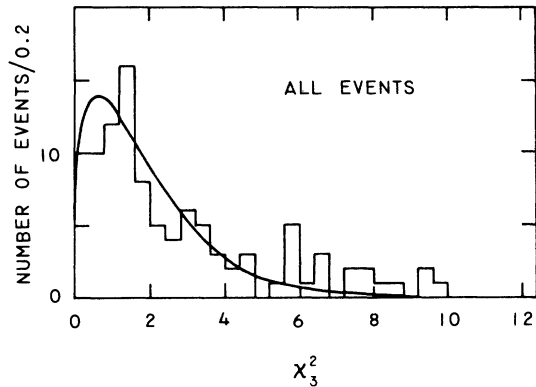


FIG. 3. Detail of the region $\chi_3^2 < 12$ for the distributions of χ_3^2 shown in Fig. 2. The superimposed curve is the expected χ^2 distribution for three degrees of freedom with a scale factor discussed in Sec. II D.

tum distribution for this sample was too large (about 1:4) to warrant further measurements.

E. Backgrounds

A small background of events in which the positive track at the primary vertex was really a proton instead of a π^+ was automatically removed by measurement of the momentum of the track. A proton of length 8 cm, the minimum acceptable track length of the π^+ , has a momentum of 300 MeV/c or more at its midpoint, so the momentum-

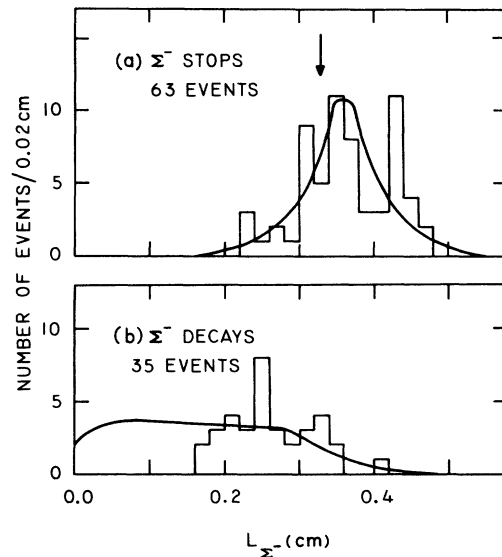


FIG. 4. Histogram of the distribution of the length of the Σ^- track, for (a) events in which the Σ^- stopped, and (b) events in which the Σ^- decayed. The curve superimposed on (a) is the resolution function for these events (see Ref. 14); the curve superimposed on (b) is the expected distribution of lengths for Σ^- which decay in flight, discussed in Sec. II F.

by-curvature measurement placed these events far off scale in Fig. 1.

In Fig. 2, an *ad hoc* flat extrapolation of the region $8 < \chi^2_3 < 32$ suggests a background of 3.5 ± 1.0 events in the sample with stopped π^+ and 8.0 ± 2.0 events in the sample with nonstopped π^+ . Such extrapolation must be justified by some physical understanding of the behavior of the background. For instance, it is not clear without some calculation whether the background from the same reaction on bound protons in carbon would increase or decrease in the region $\chi^2_3 < 8$ compared to the region $8 < \chi^2_3 < 32$. (It turns out to be decreased.)

We have obtained the same estimate, within one event, of the background both from a physical model of the sources of the background and from a more sophisticated *ad hoc* model. Since all three results agree, and the amount of background is only as large as the statistical error in the signal of 98 events, these methods are described incompletely.

The physical model attributes the background to three sources: (1) Reaction (1) in carbon with the K^- at rest; (2) unobserved decays of Σ^+ produced in carbon or hydrogen in which the associated π^- either charge-exchanged in the parent nucleus or scattered within a few millimeters and thus simulated a Σ^- -decay event; and (3) an unresolved mixture of reaction (1) from in-flight K^- interactions on either carbon or hydrogen.

Reaction (1) on carbon should be an order-of-magnitude more copious than the desired signal from reaction (1) on hydrogen, since 96% of the K^- are captured on carbon. A detailed Monte Carlo study of reaction (1) on carbon based on the impulse model discussed by Pawlewicz *et al.*⁵ led to the background curves superimposed on Figs. 1 and 2. The curves were normalized to the events in the region $130 < P_{\pi^+} < 164$ MeV/c. It is seen that this background accounts roughly for the events with $P_{\pi^+} < 160$ MeV/c and contributes no background to the sample with stopped π^+ and about 3 events to the sample with nonstopped π^+ . The contribution from this large source is small because the binding energy of the proton in carbon lowers the π^+ momentum considerably; in fact, the tail into the region near 173 MeV/c exists only because of the smearing of the π^+ momentum resulting from measurement and multiple-scattering error, effects which were built into the Monte Carlo program.

The existence of background in the uncut sample from unobserved decays of Σ^+ into π^+ is demonstrated by the peak at 184 MeV/c in Fig. 1(a), which corresponds to the momentum of a π^+ from a Σ^+ decay at rest. The three collinear events in

this peak would have been accepted as examples of reaction (1) had the π^+ not stopped, since the momentum error would then have been three times as large. Furthermore, Σ^+ decays in flight should produce a tail of background in the peak of the stopped π^+ events.

Detailed models of the unobserved Σ^+ background, the possible contribution from reaction (1) with the K^- in flight, and the background already described from reaction (1) in carbon led to an estimate of 10.0 ± 3.3 events contamination, with 2.6 in the stopped π^+ sample and 7.4 in the nonstopped π^+ sample.

Another estimate of the contamination is based on the observation that the noncollinear background, shown by the cross-hatched area in Fig. 1, is apparently independent of π^+ momentum. Therefore, it is reasonable to assume, as another *ad hoc* model, that the background which satisfies the collinearity criteria is also independent of π^+ momentum. Inside the band of momentum around 173 MeV/c which contains the acceptable events, the collinear background would be counted as true examples of reaction (1) occurring on hydrogen. Quantitative analysis of this model leads to a background estimate of 10.6 ± 1.8 events within the π^+ momentum region of acceptable events, including 3.1 events in the stopped π^+ sample and 7.5 events in the nonstopped π^+ sample.

A double check on the relative contamination of the stopped and nonstopped π^+ samples is available by analyzing the stopped π^+ sample using the momentum-by-curvature for each event instead of the momentum-by-range. In this analysis, 12% of the events acceptable as examples of reaction (1) by the use of momentum-by-curvature were rejected by the use of momentum-by-range. This fraction is consistent with the ratio of backgrounds estimated in the two samples.

As the final estimate of the background, we use 11.0 ± 2.5 events, which is roughly the average of the three methods. This leads to a correction factor of 1.130 ± 0.029 to be applied to the final rate. We find no evidence that this correction factor is different for the Σ^- -decay and Σ^- -stop events.

F. Losses and biases

The geometrical cuts on the dip (λ_{π^+}) of the π^+ , the relative azimuth ($\phi_{K^+\pi^+}$) of the K^- and π^+ , and the space angle ($\theta_{\Sigma^+\pi^-}$) between the Σ^+ and its decay π^- (for Σ^- -decay events) lead to loss factors of 0.87, 0.80, and 0.90, respectively. By examining distributions of $\sin\lambda_{\pi^+}$, $\phi_{K^+\pi^+}$, and $\theta_{K^+\pi^-}$, it was verified that these cuts were adequate to remove scanning biases against steep π^+ and nearly collinear tracks at the production or decay

vertices. All three distributions are flat within the boundaries of the cuts, having χ^2 per degree of freedom less than 1.0.

Events in which the π^+ interacts to produce a visible kink or disappear entirely before traveling 8 cm lead to a loss factor of 0.944 ± 0.014 . This factor was estimated by measuring the interaction length for such events using the copious sample of π^+ gathered in the first half of the film. This interaction length was (142 ± 35) cm, slightly higher than the geometric interaction length of 119 cm for liquid propane.¹⁵

The largest loss to be estimated is the loss of Σ^- -decay events with Σ^- -track lengths less than about 0.2 cm. For this purpose, a Monte Carlo program was written which simulated the measured length distribution of the Σ^- . Events were generated assuming a Σ^- lifetime¹⁵ of 1.484×10^{-10} sec and length smearing due to measurement error using the formula

$$\Delta L = 2\epsilon_{xv} \delta \cos\lambda(1+R^2\tan^2\lambda)^{1/2},$$

where

λ = the dip angle of the track,

$\epsilon_{xv} = 0.0145$ cm = vertex error in x or y ,

$\epsilon_{zv} = 0.0682$ cm = vertex error in z ,

$R = \epsilon_{zv}/\epsilon_{xv} = 4.71$,

$\delta = 1.3$ = empirically determined scale factor.

This formula is a good approximation to the length error assigned by TVGP.

The program predicted that 51% of the Σ^- should come to rest before decaying, at which point it is assumed that they interact with a nucleus to produce a Σ^- -stop event. Of the 49% which decay, 18% (of the total Σ^- sample) should have measured lengths greater than 0.2 cm and decay angles such that $|\cos\theta_{\Sigma\pi^-}| < 0.9$. Thus the 30 Σ^- -decay events observed with lengths greater than 0.2 cm and the 63 Σ^- -stub events represent 69% of the total sample, which is calculated to be 135 ± 14 events.

As a test that the model is consistent with our data, we note that 18% of 135 events is 24.5 events, which agrees with the 30 ± 5.5 Σ^- -decay events actually observed with Σ^- lengths greater than 0.2 cm.

The actual spectrum of lengths predicted by the Monte Carlo program is superimposed on Fig. 4(b), normalized to the 24.5 events expected with lengths greater than 0.2 cm. The curve agrees well with the data. Furthermore, if the same correction calculation is repeated, using a cut of 0.24 cm on the Σ^- length, the same estimate of 135 events for the total sample is obtained.

A further loss of $(1 \pm 1)\%$ of the events is expected from the cut $K_t < 3.0$. As a final check against biases, we note that the fraction of events after background subtractions with a stopped π^+ is 0.65 ± 0.05 , compared to the value of 0.57 ± 0.04 measured for the momentum interval 162–182 MeV/c using the large sample of $\pi^+\pi^-$ events.

A summary of loss factors which apply to the entire sample appears in Table I.

G. Number of stopped K^-

The number of beam tracks interacting in the fiducial volume was counted on every twentieth frame, subject to the two cuts mentioned in Sec. IIA. Multiplying this count by 20, we conclude that there were $17\,800 \pm 595$ interacting K^- in the film scanned. Pion contamination in the small fiducial volume was negligible; however, the above number must be corrected for in-flight K^- interactions and decays.

The K_t distribution¹³ for the beam tracks of 604 events is displayed in Fig. 5. This distribution should have a mean of zero and a variance of one for a pure sample of stopped K^- . The long tail on the positive side corresponds to K^- interactions in flight. Since the tail of the stopped K^- extends only to $K_t \approx -3.0$, we can assume (by symmetry) that all the events with $K_t > 3.0$ are in-flight interactions. This pure background must be extrapolated into the region $K_t < 3.0$ (corresponding to momenta less than 210 MeV/c) to deduce the in-flight contamination under the peak of stopped K^- .

The events entering Fig. 5 were the measured sample of topologies (2), (3), and (4) in the first half of the film, most of which must originate from the reaction $K^-p \rightarrow \Sigma^- \pi^+$ either in carbon or hydrogen. To extrapolate the background, we have assumed that the momentum dependence of

TABLE I. Loss factors applicable to the entire sample of reaction (1). The left-hand column describes the cut responsible for the loss factor in the right-hand column.

Source	Factor
Dip $\pi^+ < 60^\circ$	0.867
$18^\circ < \phi_{K\pi} < 162^\circ$	0.800
Length $\pi^+ > 8$ cm	0.944 ± 0.014
Scan efficiency	0.938 ± 0.028
Background	1.130 ± 0.029
$K_t < 3$	0.990 ± 0.010
$\chi^2_3 < 8$	0.995 ± 0.002
Total	0.680 ± 0.030

the cross section for this reaction is the same on carbon as on hydrogen, for which the cross section has been measured¹⁶ at momenta as low as 50 MeV/c. An empirical fit to the measured cross sections as a function of momentum was transformed to a distribution of interaction rate as a function of K_t , using the range-momentum relationship and an empirically determined relationship between K_t and the momentum:

$$P = 154K_t^{0.285},$$

where P is the K^- momentum at interaction in MeV/c. The resulting distribution was smeared in a Gaussian manner to simulate the multiple scattering error in K_t and normalized to the region $3 < K_t < 6$, resulting in the solid curve in Fig. 5. The normalization region in the variable K_t corresponds to the K^- momentum region $210 < P < 260$ MeV/c, below which the data begin to include stopped K^- and above which the scanning cut with the curvature template removed most events.

This model predicts an in-flight background of 97 events in the region $K_t < 3.0$. The distribution of K_t with background subtracted, displayed on the Fig. 5 insert, is symmetric about $K_t = -0.25$ rather than $K_t = 0$ as it should be. The distribution of K_t is sensitive to the calibration of the density of the propane which enters into the range-momentum relationship, and the observed shift is consistent with the uncertainty in this calibration.

The above extrapolation cannot be directly applied to the beam track count because this count included all K^- interactions, some of which have cross sections whose momentum dependence is quite different from the $\Sigma^- \pi^+$ channel. For example, the cross section for the reaction $K^- p \rightarrow \Sigma^+ \pi^-$, which has a much weaker momentum dependence than the $\Sigma^- \pi^+$ channel,¹⁶ would lead to a background curve shown as dashes in Fig. 5 and predict a background subtraction of 62 events.

These two final states represent the extremes in the momentum dependence of cross sections for all $K^- p$ reactions. Therefore, we take the average of the curves as the background subtraction in the region $K_t < 3.0$ and attach an error to this estimate which is half the difference between the two curves. There is also a statistical error of about the same size, which is added in quadrature, resulting from the normalization of the curves to the 36 events in the region $3 < K_t < 6$. The conclusion is that the fraction of beam tracks which interact at rest is $f = 0.79 \pm 0.04$.

The same model was applied to a sample of 500 events with final states containing a Λ and no π^+ , in the same fiducial volume, with the result

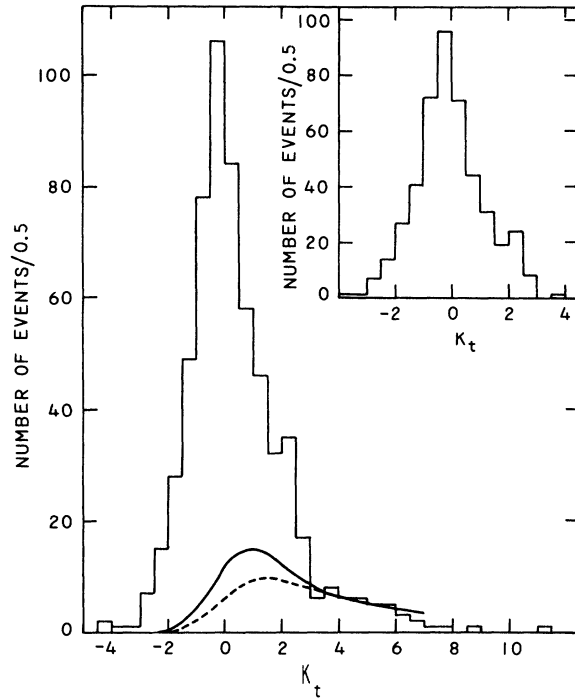


FIG. 5. Histogram of the distribution of K_t for the K^- track (see Ref. 13), for 604 events belonging to topologies (2), (3), and (4) from the first half of the measured film. The inset shows the same distribution after subtraction of the solid background curve. The models leading to the two background curves superimposed on the histogram are discussed in Sec. II G.

$$f = 0.75 \pm 0.04.$$

An additional subtraction of $(5 \pm 1)\%$ must be made for K^- decays in flight. This number was calculated using the known spectrum of K^- momenta at the entrance to the fiducial volume, the range-momentum relationship, and a K^- lifetime¹⁵ of 1.237×10^{-8} sec. The final estimate of the number of stopped K^- in this experiment is 13400 ± 840 .

III. RESULT

The branching ratio for reaction (1) on free protons has been taken to be 0.459 ± 0.006 .¹⁷ The fraction of stopped K^- which interact with free protons can then be calculated, using the corrected number of events detected (135 ± 14), the detection efficiency (0.680 ± 0.030), and the number of stopped K^- (13400 ± 835). The result is

$$R = 0.0323 \pm 0.0042.$$

The error in R includes all systematic errors which we have considered. The statistical error alone would be ± 0.0032 .

IV. CONCLUSIONS

VanderVelde-Wilquet *et al.*⁶ have also measured this capture fraction in a mixture of hydrocarbons which was mostly C_3H_8 , with the result $R=0.040 \pm 0.004$ with a possible systematic error of ± 0.005 , in addition to the quoted statistical error. Our result is in good agreement with theirs.

The modification proposed by Pawlewicz *et al.*⁵ to the large-mesonic-molecule model of Ponomarev⁴ was that the probability of final interaction on a hydrogen nucleus in a molecule Z_mH_n is given by

$$W = \frac{A_L}{Z^2} \frac{n}{mZ+n} (1-P_t),$$

where P_t is the probability that the captured negative particle transfers from hydrogen to the heavy nucleus during the cascade process, and A_L is a proportionality constant which is expected

to depend only on the location of the element Z in the Periodic Table.

If the extreme assumption is made that P_t is zero for antiprotons, then A_L is 12.9 ± 3.5 for C_3H_8 , using the result of Pawlewicz *et al.*¹⁸ Our measurement of W for K^- then implies that P_t is $(71 \pm 9)\%$ for K^- . W for π^- has not been measured for propane; however, Krumshtein *et al.*³ found W to be $(1.90 \pm 0.22)\%$ for π^- in C_7H_{16} , a molecule very similar in structure to C_3H_8 , leading to a value of $(81 \pm 6)\%$ for P_t for π^- . All of these estimates of P_t are lower limits, since P_t was assumed to be zero for antiprotons.

ACKNOWLEDGMENTS

We are indebted to U. Sevick and the crew of the 40-in. bubble chamber for their efforts in producing the exposure. We thank Carrie Yates and Harold Scheller for the scanning and measuring.

*Work supported by the U. S. Atomic Energy Commission.

†Present address: National Accelerator Laboratory, Batavia, Illinois 60510.

‡Present address: 201 Maniktala Main Road, Calcutta-54, India.

¹W. K. H. Panofsky, R. Aamodt, and J. Hadley, *Phys. Rev.* **81** (1951).

²E. Fermi and E. Teller, *Phys. Rev.* **72**, 399 (1947).

³Z. V. Krumshtein, V. I. Petrukhin, L. I. Ponomarev, and Yu. D. Prokoshkin, *Zh. Eksp. Teor. Fiz.* **54**, 1690 (1968) [*Sov. Phys.—JETP* **27**, 906 (1968)].

⁴L. I. Ponomarev, *Yad. Fiz.* **2**, 223 (1965) [*Sov. J. Nucl. Phys.* **2**, 160 (1966)]; **6**, 389 (1967) [*Sov. J. Nucl. Phys.* **6**, 281 (1968)].

⁵W. T. Pawlewicz, C. T. Murphy, J. G. Fetkovich, T. Dombeck, M. Derrick, and T. Wangler, *Phys. Rev. D* **2**, 2538 (1970).

⁶C. VanderVelde-Wilquet, G. S. Keyes, J. Sacton, J. H. Wickens, D. H. Davis, and D. N. Tovee, *Nuovo Cimento Lett.* **5**, 1099 (1972).

⁷For further details on the film, beam, and chamber, see M. Saha, J. G. Fetkovich, W. Heintzelman, C. Mel-tzer, and C. T. Murphy, *Phys. Rev. D* **7**, 3295 (1973).

⁸A Σ^- which is captured by carbon and produces a Λ can also produce "boil-off" protons as the carbon nucleus breaks up.

⁹F. T. Solmitz, A. D. Johnson, and T. B. Day, Alvarez Group, Lawrence Radiation Laboratory Programmer's Note. No. P-117, 1965 (unpublished).

¹⁰The most important criteria required that the rms deviation of the spiral fit to the K^- and π^+ tracks be less than 50 microns on the film and that the χ^2 per

degree of freedom for the reconstruction of the vertices be less than 6.

¹¹R. M. Sternheimer, *Phys. Rev.* **117**, 485 (1960).

¹²C. T. Murphy, Univ. of Michigan Bubble-Chamber Group Research Note No. 65/67, 1966 (unpublished).

¹³ K_t is defined by the equation $K_t = (k_r - k_c)/\Delta k_c$, where k_c is the inverse of the momentum at the track center as measured by the spiral fit of TVGP, Δk_c is its error, and k_r is the inverse of the momentum at the center calculated from the range of the track, assuming that it came to rest at the end.

¹⁴The resolution function is the Gaussian ideogram of the errors in the lengths of each event, all centered at 0.36 cm.

¹⁵Particle Data Group, *Rev. Mod. Phys.* **45**, S1 (1973).

¹⁶W. E. Humphrey and R. R. Ross, *Phys. Rev.* **127**, 1305 (1962); M. Sakitt, T. B. Day, R. G. Glasser, N. Seeman, J. Friedman, W. E. Humphrey, and R. R. Ross, *Phys. Rev.* **139B**, 719 (1965); M. Ferro-Luzzi, R. D. Tripp, and M. Watson, *Phys. Rev. Lett.* **8**, 28 (1962); P. Nordin, Jr., *Phys. Rev.* **123**, 2168 (1961).

¹⁷This is the same value as that used in Ref. 6. It is calculated from the charged-to-neutral-hyperon production ratio measured by Humphrey and Ross (Ref. 16) and the ratio of Σ^+ to Σ^- production obtained in emulsion by D. N. Tovee, D. H. Davis, J. Simonovic, G. Bohm, J. Klabuhn, F. Wysotzki, M. Csejthey-Barth, J. H. Wickens, T. Cantwell, C. Ni Ghogain, A. Montwill, K. Garbowska-Pniewska, T. Pniewski, and J. Zakrzewski, *Nucl. Phys.* **33B**, 493 (1971).

¹⁸See Ref. 5. The value of A_L deduced in Ref. 5 is incorrect.